




Bulk organic geochemical and palynofacies analyses of the Hettangian Datta Formation (Potwar Basin, Pakistan): Regional comparison with the time equivalent Lathi Formation (Jaisalmer Basin, India)

NASAR KHAN^{1,2,3,*} , IRFAN U JAN^{3,6}, SHAHID IQBAL^{4,5}, RUDY SWENNEN¹, OSMAN SALAD HERSI⁶ and HAFIZ S HUSSAIN^{2,7}

¹Department of Earth and Environmental Sciences, KU Leuven, Leuven 3001, Belgium.

²Department of Geology, University of Malakand, Chakdara 18800, Pakistan.

³National Centre of Excellence in Geology, University of Peshawar, Peshawar 25130, Pakistan.

⁴Department of Earth Sciences, Quaid-i-Azam University, Islamabad 45320, Pakistan.

⁵Department of Geodynamics and Sedimentology, University of Vienna, Vienna, Austria.

⁶Department of Geology, University of Regina, Saskatchewan, Canada.

⁷Department of Earth and Planetary Sciences, Macquarie University, Macquarie Park 2109, Australia.

*Corresponding author. e-mail: nasar_khan@uom.edu.pk

MS received 3 December 2020; revised 22 March 2021; accepted 23 March 2021

A detailed lithostratigraphic, bulk organic geochemical and palynofacies analyses were performed on organic-rich shale and coal samples from the Hettangian Datta Formation in the western Salt Range, southern Potwar Basin, Pakistan, to evaluate its hydrocarbon generation potential. Organic matter (OM) in the formation is mainly dominated by gas-prone Type III kerogen and oil- and gas-prone Type II kerogen. The coal and OM-rich shale intervals are thermally mature, while grey shale intervals are thermally immature. Palynofacies studies showed that the Datta Formation is rich in inertinite, vitrinite and amorphinite with minor liptinite. The OM is mainly of terrigenous origin with minor marine contribution and is interpreted to have been deposited under suboxic to anoxic conditions in a fluvio-deltaic depositional setting. The thermal maturity estimated from Spore Colour Index (SCI) and Thermal Alteration Index (TAI) was entirely consistent with estimates based on bulk organic geochemical data. Variations in thermal maturity are interpreted to be due to change in kerogen types as well as burial depth. Overall, the organic geochemical and palynofacies studies showed that the coal and OM-rich shale intervals in the Datta Formation have good-to-excellent source rock potential in the study area, whereas the grey shale intervals have poor potential as source rocks. The Datta Formation has tentatively been correlated with the stratigraphically equivalent Lathi Formation in the Jaisalmer Basin, India, which was deposited in a similar palaeo-depositional setting on the NW margin of the Indian Plate affected by Neo-Tethys realms.

Keywords. Jurassic; organic matter; hydrocarbon; thermal maturity; source rock.

1. Introduction

Exploration activities in the Potwar Basin (figure 1), Pakistan, began almost a century ago and a number of oil- and gas-fields have since been discovered (Kadri 1995; Asif *et al.* 2014; Craig *et al.* 2018), but the origin of the hydrocarbons is still the subject of debate. It has widely been assumed that the Upper Paleocene Patala Formation represents a source rock for most of the Potwar Basin reservoirs, but recent studies have suggested that the Lower Jurassic Datta Formation may also act as source rock in a number of oil fields (e.g., Fazeelat *et al.* 2010; Asif and Fazeelat 2012; Zaidi *et al.* 2013; Khan 2016; figure 2). The Hettangian Datta Formation (~400 m thick) includes both continental and marine sediments (Shah 2009) and consists of near-shore siliciclastic and minor carbonate sediments with organic-rich shale and coal intervals (Abbasi *et al.* 2012; Iqbal *et al.* 2015; Craig *et al.* 2018; figure 3A–F). The formation has been studied in terms of sedimentology, biostratigraphy and sequence stratigraphy in the Potwar, Kohat and Hazara basins of Pakistan (Ashraf *et al.* 1976; Mujtaba and Memon 1990; Abbasi *et al.* 2012; Ahmad *et al.* 2013; Iqbal *et al.* 2015, 2019), but has received only limited attention in terms of its source rock potential evaluation and regional comparison. The recent discoveries of hydrocarbons in Datta Formation reservoirs at the Dhulian, Meyal, Balkasar, Makori, and Manzali

oil/gas fields of Pakistan have encouraged further detailed source and reservoir studies in the Potwar Basin (Asif and Fazeelat 2012; Khan 2016; Craig *et al.* 2018).

This paper investigates the source rock potential of the OM-rich shale and coaly intervals in the Lower Jurassic Datta Formation of Potwar Basin. Previous source rock studies of the Datta Formation have been based mostly on TOC (total organic carbon) and Rock-Eval pyrolysis. However, palynofacies studies, which are a focus of this paper, have been lacking (Ahmed and Alam 2007; Asif and Fazeelat 2012; Asif *et al.* 2014). In addition, kerogen types, abundance of organic matter, thermal maturity and palaeo-depositional environment for the Datta Formation are also assessed in this study.

Recent sedimentological studies of the Datta Formation include Abbasi *et al.* (2012) and Iqbal *et al.* (2015). Abbasi *et al.* (2012) identified four distinct lithofacies in the formation in the western Salt Range (channel belt, floodplain, swamp and lagoon) of which the latter two contain coal beds and OM-rich shales. In this study, these were selected as suitable lithologies for source rock characterization. To broaden the context of this study, the formation has tentatively been correlated with the stratigraphically equivalent Lathi Formation in the nearby Jaisalmer Basin in western Rajasthan of NW India (figure 4A, B). Palaeogeographically, the Potwar and Jaisalmer basins

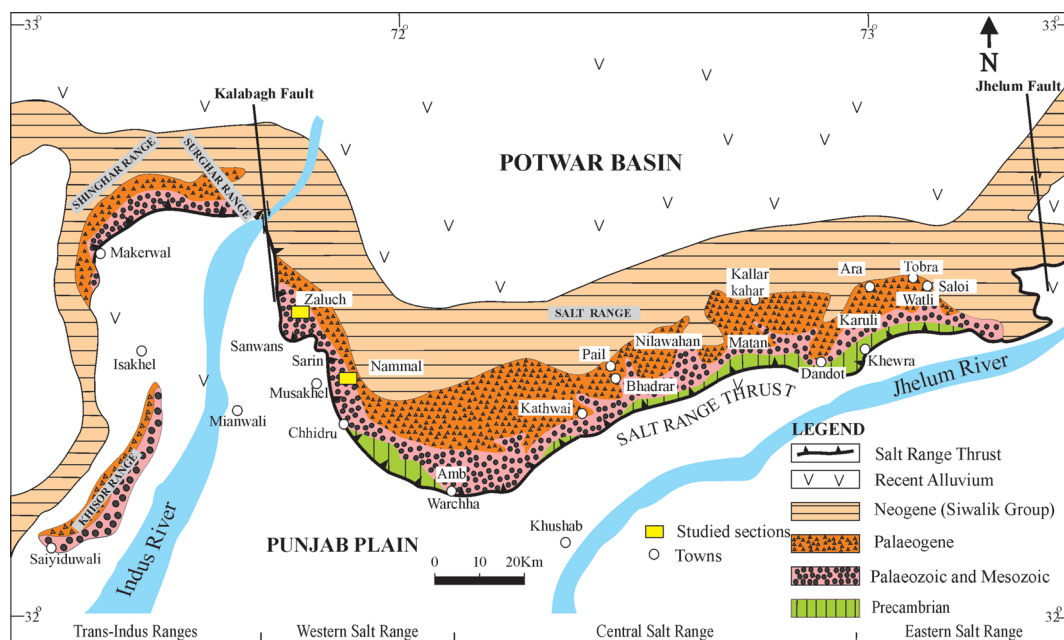


Figure 1. Geologic map of the Potwar Basin illustrating location and tectonic setting of the study areas (i.e., Salt Range; measured sections are (1) Nammal Gorge section and (2) Zaluch Nala section) (modified after Jan *et al.* 2016).

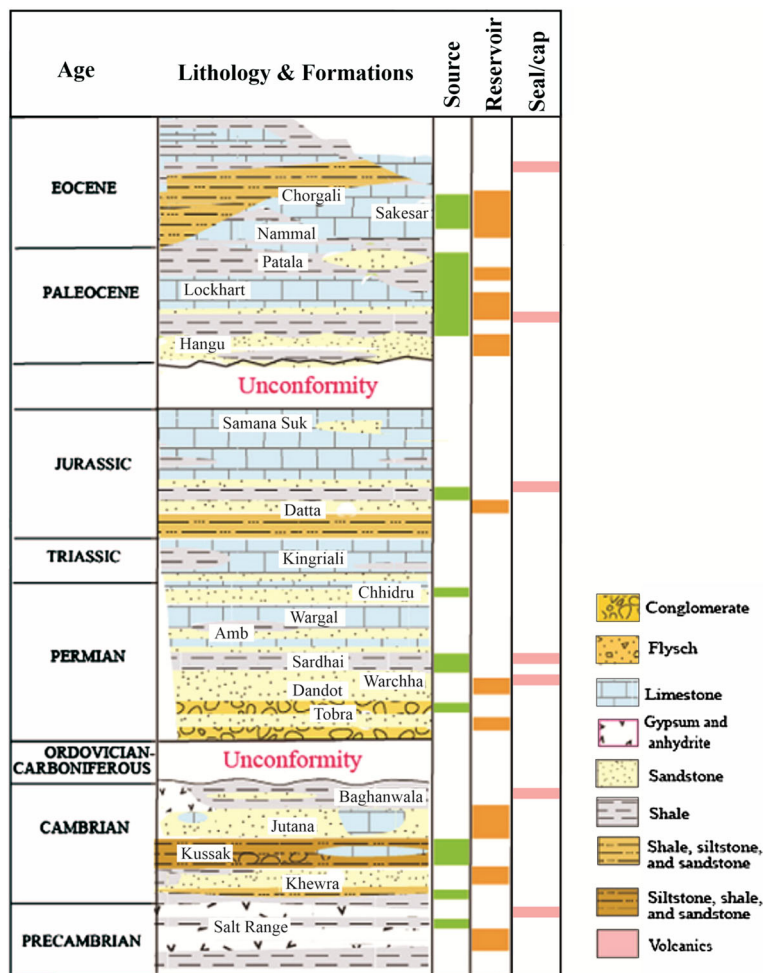


Figure 2. Lithostratigraphy and geologic formations providing elements for petroleum system in the Potwar Basin (after Wandrey *et al.* 2004; Shah 2009).

are both located in the Indian Plate and their Lower Jurassic successions are assumed to have been deposited at the southern margin of Neo-Tethys under similar depositional, biogeochemical and geomorphological conditions (Kazmi and Jan 1997; Golonka 2007; Iqbal *et al.* 2015; Craig *et al.* 2018; figure 4A, B). Thus, palaeo-geographic setting of the Potwar and Jaisalmer basins have been reconstructed to develop a regional comparison between Datta and Lathi formations.

2. Tectono-stratigraphic setting

In Early Mesozoic, the Pangaea split into two supercontinents of Laurasia (north) and Gondwanaland (south); they were separated by the Tethys Ocean (Kazmi and Jan 1997; Rees *et al.* 2000; Ali and Aitchison 2008; figure 4A). Through most of the Mesozoic Era, the Indian Plate (study area is part of it) remained part of Gondwanaland

and the Tethys Ocean (Kazmi and Abbasi 2008; figure 4A, B). In Late Triassic Period, the sea regressed resulting in sedimentation gap and erosion, followed by deposition of fluvial to deltaic sediments (Datta Formation) in Early Jurassic (Abbasi *et al.* 2012; Iqbal *et al.* 2019). Consequently, the Indian Plate separated from Gondwanaland in Early Cretaceous Period, drifted northwards and eventually the Neo-Tethys subducted beneath the Eurasian Plate and collided with remnant Kohistan–Ladakh Arc (Kazmi and Jan 1997; Ali and Aitchison 2008). The drifting continued and Indian Plate collided with the Eurasian Plate (about 52 Ma). As a consequence of northward movement of Indian Plate, the marine sediments were compressed and crumpled and then squeezed up to form the Himalayas Mountains (Kazmi and Jan 1997; Baker *et al.* 1988). This collision resulted in the development of a number of thrust faults in Pakistan, including (from north to south) the Main Karakorum Thrust (MKT),

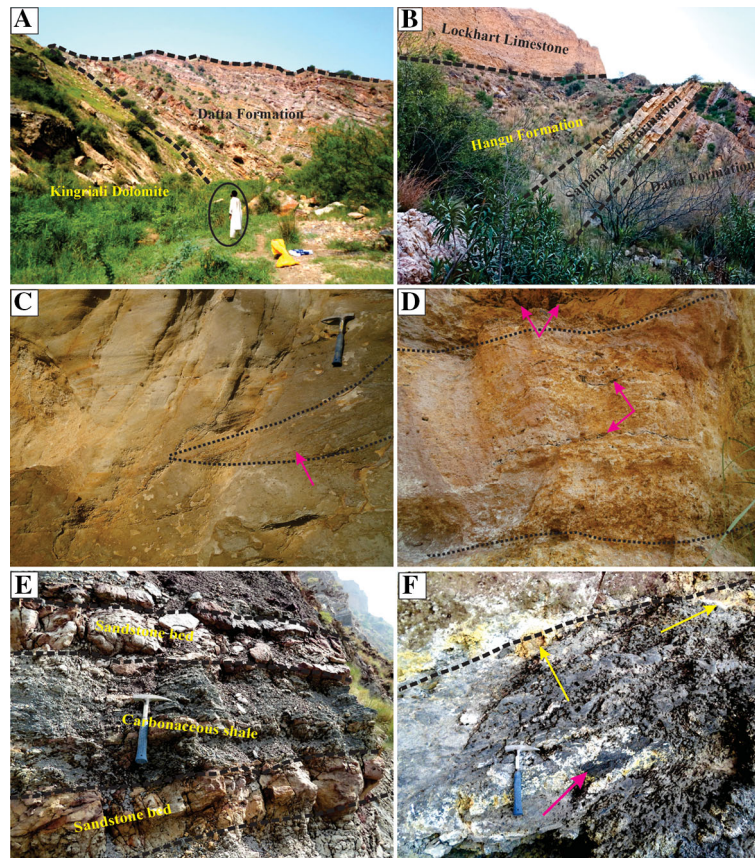


Figure 3. Field photos of the Hettangian Datta Formation. (A) Lower contact (disconformable) with Triassic Kingriali Formation; (B) upper contact (disconformable) with Middle Jurassic Samana Suk Formation; (C) sandstone lithofacies having cross beds (pink arrow); (D) conglomeratic lithofacies having reworked coal patches (pink arrows) and pebbles; (E) carbonaceous shale beds interbedded with fine grained sandstone lithofacies; and (F) coal lithofacies with coaly clasts (pink arrow) overlain by sandstone lithofacies. The yellow arrows show pyrite mineralization associated with coals.

Main Mantle Thrust (MMT), Main Boundary Thrust (MBT) and the Salt Range Thrust (SRT) (Baker *et al.* 1988; Kazmi and Jan 1997; Grelaud *et al.* 2002). The later thrust exposed most of the older sediments at various outcrop sections in the Potwar Basin (figure 1).

Palaeo-geographically, the Potwar Basin was located on the north-western margin of the Indian Plate having affinity with Neo-Tethys realm during Early Jurassic time and holds the depositional record from Late Proterozoic to Holocene (Rees *et al.* 2000; Shah 2009; Iqbal *et al.* 2019; figure 4A, B). The study area of this paper lies in the Salt Range area which occurs at the southern part of the Potwar Basin (figure 1). Geologically, Salt Range is the southernmost edge of the Himalayan foreland fold-and-thrust belt, formed as a result of Indian and Eurasian plates collision and is bounded by Potwar Plateau to the north, the SRT to the south, the Jhelum Fault to the east and consequently the Kalabagh Fault to the west (Grelaud *et al.* 2002; Wandrey *et al.* 2004; figure 1).

Progressive deformation associated with the Himalayan Orogeny has resulted in the development of anticlinal, pop-up, salt diapiric and stratigraphic traps in the Potwar Basin, features that are integral for development of petroleum systems (Kadri 1995; Craig *et al.* 2018).

The Mesozoic sedimentary section in the Salt Range is about 1000 m thick and is composed of mixed siliciclastics and carbonates deposited along the SW margin of the Neo-Tethys Ocean during the break-up of Gondwanaland (Kadri 1995; Kazmi and Abbasi 2008; Craig *et al.* 2018). Lower Jurassic sediments in the Potwar Basin are dominated by the nearshore siliciclastics of the Datta Formation, the mixed clastic and carbonate facies of the Shinawari Formation (Middle Jurassic), and the carbonates of the Samana Suk Formation (Middle Jurassic), while Upper Jurassic strata are missing (Abbasi *et al.* 2012; Craig *et al.* 2018; figure 2). Eastwards in the Salt Range and the Potwar Basin, Jurassic rocks were thinned and eroded during pre-Cenozoic uplift; however, they

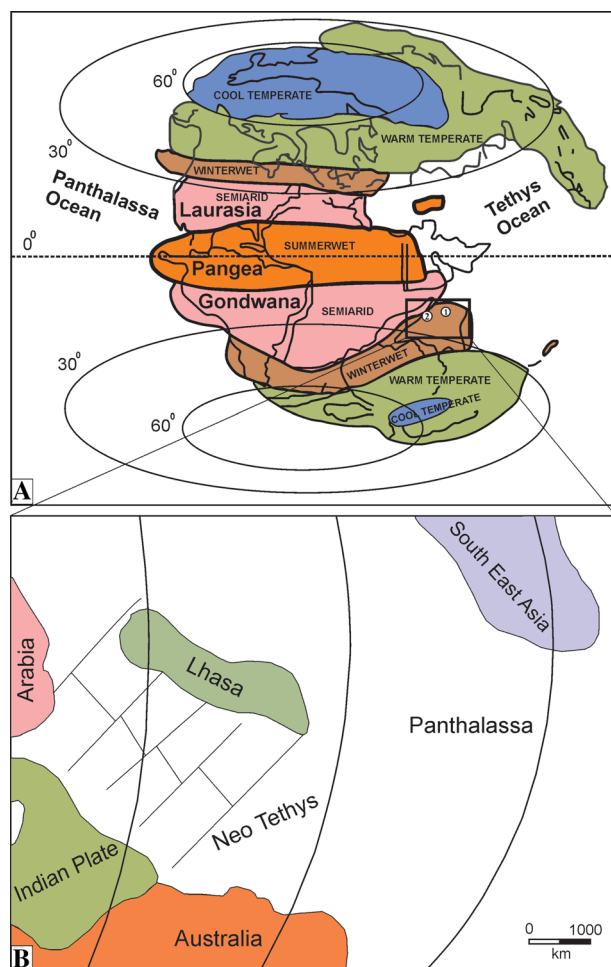


Figure 4. (A) Palaeogeographic map showing location of (1) Potwar Basin, Pakistan and (2) Jaisalmer Basin, India during Early Jurassic Period with prevailed climatic zones (after Rees *et al.* 2000; Iqbal *et al.* 2019). (B) Reconstructed palaeogeographic map displaying position of Indian Plate surrounded by Neo-Tethys during Early Jurassic (Golonka 2007).

thicken towards the west in the Potwar and Kohat basins (Kazmi and Abbasi 2008; Abbasi *et al.* 2012; Craig *et al.* 2018). A number of major unconformities are also reported and show the absence (due to either erosion or non-deposition) of Ordovician to Carboniferous, Late Cretaceous and Oligocene strata of the Gondwanaland sedimentation in the Potwar Basin of Pakistan (Shah 2009; Craig *et al.* 2018; figure 2).

3. Dataset and methodology

The study is primarily based on fieldwork and laboratory analyses of the organic-rich sediments of Datta Formation exposed at the Nammal Gorge (N: 32°39'54.03", E: 71°48'07.04") and Zaluch Nala (N: 32°46'53.21", E: 71°38'33.62") sections in the western Salt Range, Potwar Basin of Pakistan

(figure 1). Lithostratigraphic sections were measured, logged, photographed and sampled following standard field methods (Tucker 2003; figures 3A–F, 5 and 6). Marker horizons such as, erosional surfaces, oxidized, rippled, bioturbated and cross-bedded intervals were recorded. A total of 40 rock samples were collected, from which 20 representative samples were selected for laboratory analyses covering a wide range of lithologies, sedimentary textures and organic richness. Weathered and eroded surfaces at the outcrop were removed and rock samples were collected from fresh surfaces to avoid OM degradation (Tyson 1995; Khan *et al.* 2018). The laboratory analyses performed include bulk organic geochemical, palynofacies and spore colour index/thermal alteration index (SCI/TAI) analyses.

3.1 Bulk organic geochemical analyses

The bulk organic geochemical analyses, including TOC (total organic carbon) content and Rock-Eval pyrolysis, were performed in the Laboratory of Petroleum Geology, National Centre of Excellence in Geology (NCEG), University of Peshawar and in the Laboratory of Hydrocarbon Development Institute of Pakistan, respectively. An Eltra CW800 analyzer was used for TOC analysis and samples with TOC > 0.5 wt.% were screened for Rock-Eval pyrolysis and palynofacies analyses.

The Rock-Eval pyrolysis was performed using Rock-Eval 6 pyrolyser (latest of version of Vinci Technologies) by heating a 100 mg of crushed, bulk rock sample in a helium atmosphere under programmed heating (up to 650°C) following standard methods (Hunt 1995; Béhar *et al.* 2001). The parameters measured included S₁ (the free hydrocarbons in mg HC/g rock), S₂ (the cracked hydrocarbons in mg HC/g rock), S₃ (the carbon- and oxygen-containing compounds in mg CO₂/g rock), and the temperature of maximum pyrolysis (T_{max}) which was used to estimate the thermal maturity of the organic matter (van-Krevelen 1993; Hunt 1995). For evaluation of the source rock potential, the hydrogen index (HI), oxygen index (OI) and production index (PI) were calculated and compared with published standards (table 1).

3.2 Palynofacies analysis

Palynological maceration was carried out on 20 rock samples using standard preparation methods (Tyson 1995; Traverse 2007). The samples were

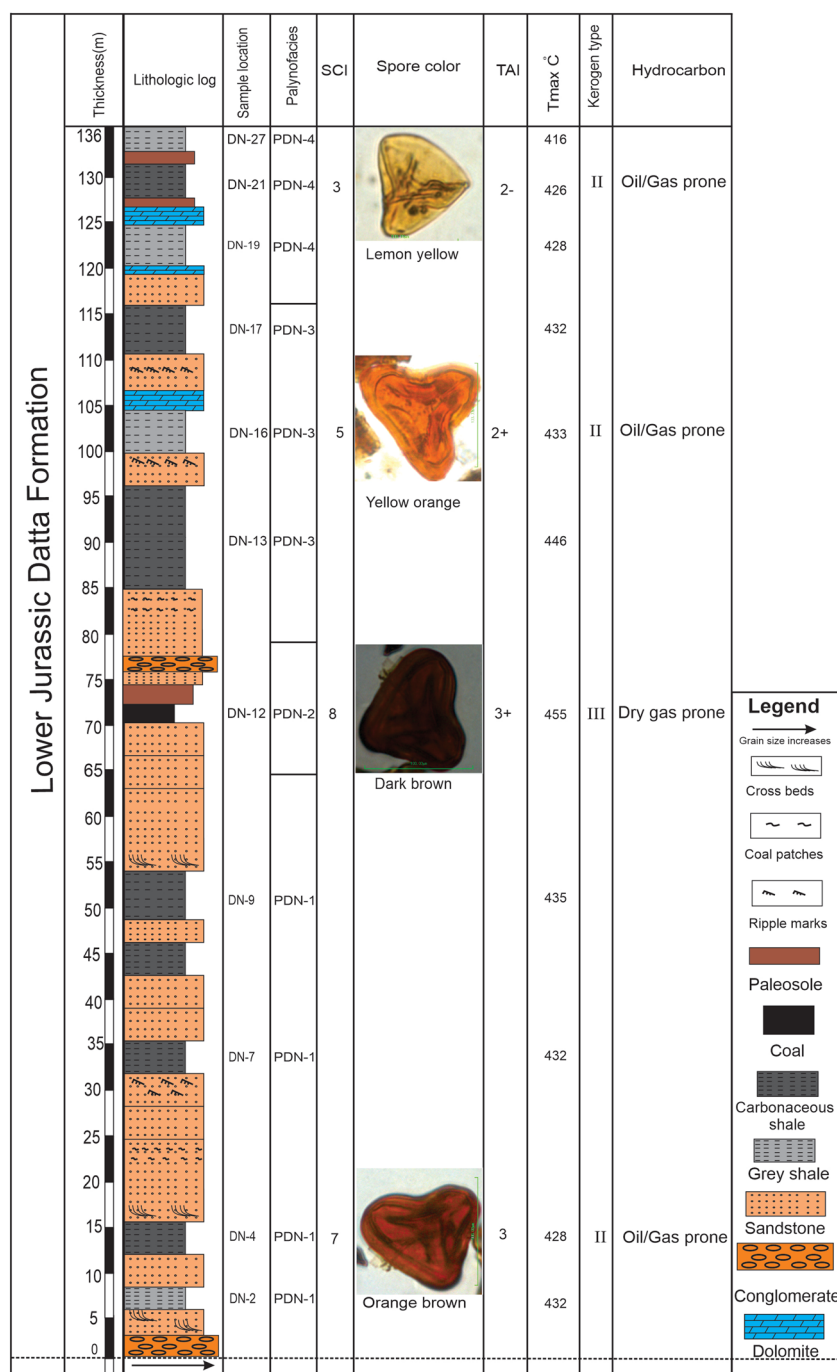


Figure 5. Lithologic log of the Datta Formation at Nammal Gorge section presenting spore colour index, palynofacies types, kerogen types and expected hydrocarbons of the analysed intervals. The change in spore colour indicates an increase in thermal maturity with change in colour from lemon yellow to orange brown.

first treated with 20% concentrated hydrochloric acid and 60% hydrofluoric acid to dissolve carbonates and silicates, respectively. The samples were then neutralized and centrifuged in ZnCl₂ solution to remove heavy minerals, leaving only organic matter (OM) as a residue. The organic residue was sieved through 10 μm nylon mesh and was mounted on glass slides using liquid elvacite. A Nikon LV-100-ND microscope equipped with

digital camera was used for photo-microscopy at the Laboratory of Sedimentology and Palynology, University of Peshawar. A total of 300 counts of organic components were made per sample and their percentage distributions were calculated for palynofacies classification and quantitative measurements of organic macerals following Tyson (1995) and Ghasemi-Nejad *et al.* (2009). Likewise, for qualitative and quantitative analysis of

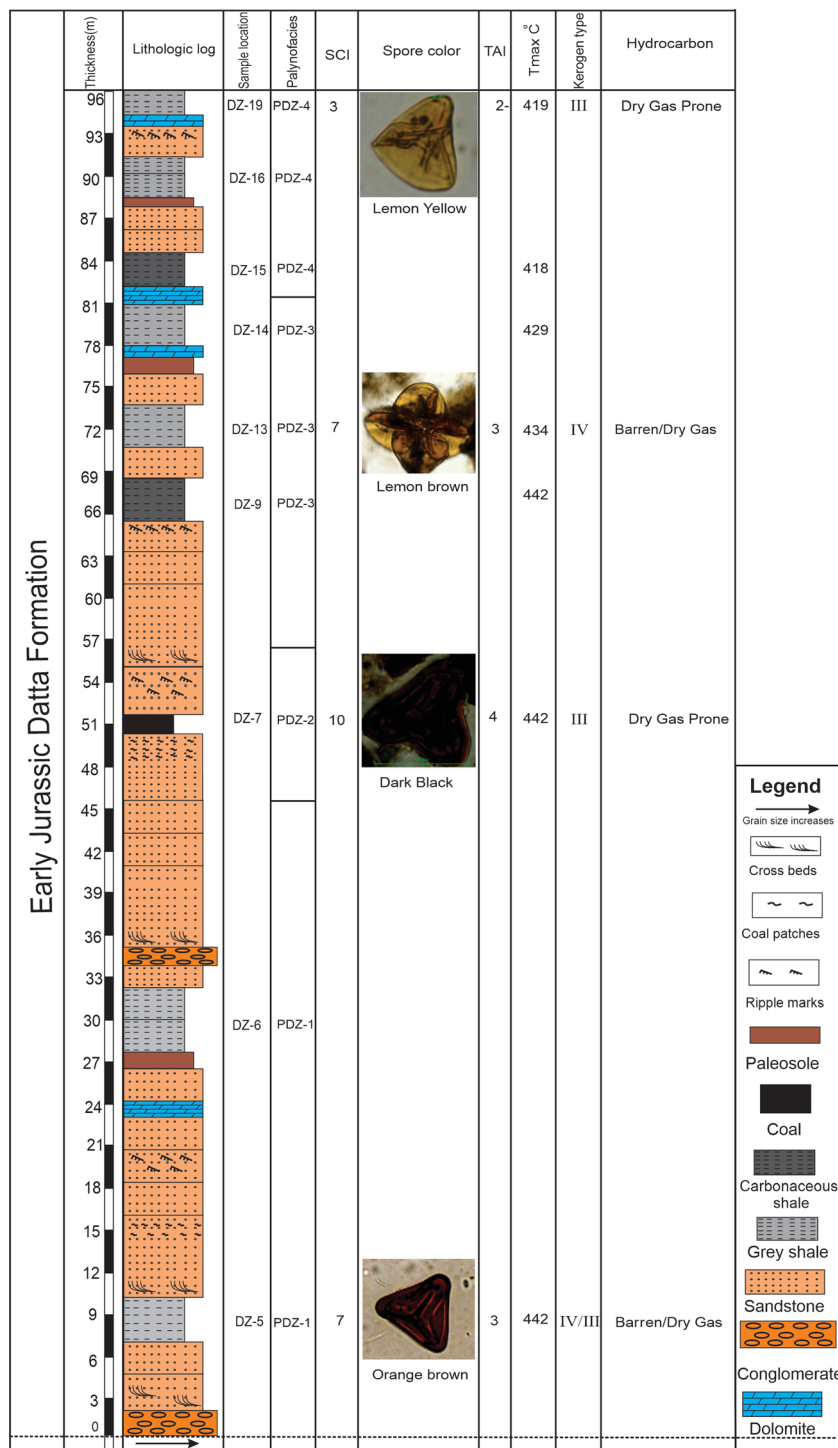


Figure 6. Lithologic log of the formation at Zaluch Nala section illustrating spore colour index, palynofacies types, kerogen types and expected hydrocarbon types of the analysed intervals. The change in spore colour indicates an increase in thermal maturity with change in colour from lemon yellow to orange brown.

kerogen macerals including inertinite, vitrinite, amorphinite and liptinite, the guidelines suggested by Tyson (1995), Ercegovac and Kostic (2006) and Filho *et al.* (2012) along with some terminologies from Zoba *et al.* (2013), El-Diasty *et al.* (2017) and Khan *et al.* (2018) were used in this study.

3.3 Spore colour index and thermal alteration index (SCI/TAI)

The colour of palynomorphs changes as a function of progressive change in temperature, burial depth and maturation time and is expressed as SCI or TAI (Filho *et al.* 2012; Zhang *et al.* 2015). In this

Table 1. Rock-Eval pyrolysis outcomes of the formation at studied sections: S_1 (free hydrocarbon (HC), mg HC/g rock), S_2 (cracked HC), S_3 (Carbon dioxide yield, mg CO_2 /g rock), GP (Genetic Potential), HI (Hydrogen Index), TOC (Total Organic Carbon, wt.%), T_{max} (temperature at maximum of S_2 peak), PI (Production Index), OI (Oxygen Index, mg CO_2 /g TOC).

Sections	Sample no.	TOC (wt.%)	Rock-Eval pyrolysis						T_{max} ($^{\circ}C$)	
			S_1	S_2	S_3	GP	HI	OI		PI
Nammal Gorge section	DN-27	0.62	0.05	0.51	0.55	0.56	82.26	88.71	0.09	416
	DN-21	1.12	0.24	2.66	0.91	2.9	237.5	81.25	0.08	426
	DN-19	1.51	0.06	4.69	1.32	4.86	315.14	86.17	0.03	428
	DN-17	1.64	0.26	2.68	0.82	2.94	163.41	50	0.08	432
	DN-16	6.23	1.47	20.62	3.43	21.98	329.9	55.32	0.07	433
	DN-13	4.22	1.22	8.22	2.33	9.44	194.78	55.21	0.12	446
	DN-12	12.5	4.22	78.45	9.04	82.67	627.6	72.32	0.05	455
	DN-9	1.88	0.26	6.22	1.44	6.48	330.85	76.6	0.04	435
	DN-7	1.52	0.07	4.79	1.31	4.86	315.13	86.18	0.01	432
	DN-4	0.82	0.08	0.48	0.56	0.28	58.54	68.29	0.31	426
	DN-2	0.45	–	–	–	–	–	–	–	–
Average	=	2.96	0.79	12.93	2.17	13.7	265.51	72.01	0.08	432.9
Zaluch Nala section	DZ-19	0.58	0.02	0.82	0.36	0.84	141.38	62.07	0.02	415
	DZ-16	0.44	–	–	–	–	–	–	–	–
	DZ-15	1.22	0.04	4.22	0.31	4.26	345.9	25.41	0.01	418
	DZ-14	0.82	0.08	0.20	0.26	0.28	24.39	31.7	0.28	429
	DZ-13	1.12	0.06	3.22	2.15	3.28	287.5	191.96	0.02	434
	DZ-9	6.22	2.54	20.84	17.74	17.38	321.54	279.42	0.1	438
	DZ-7	8.32	3.78	70.1	30.74	73.88	842.55	369.47	0.05	442
	DZ-6	0.46	–	–	–	–	–	–	–	–
	DZ-5	0.52	0.04	0.21	0.33	0.25	40.38	63.46	0.16	442
Average	=	2.19	0.94	14.23	7.42	14.31	286.23	146.21	0.09	431.14

method, three specific palynomorph species, *Deltoideospora*, *Classopollis torosus* and *Trilobosporites laevigatus* were utilized and their colours were matched with standard colour charts of SCI and TAI following Pross *et al.* (2007), Filho *et al.* (2012) and Koch *et al.* (2017). This approach was used to assess the visual and qualitative thermal maturity of the OM encountered within the investigated formation.

4. Results

4.1 Lithostratigraphy

In the study area, the Hettangian Datta Formation rests unconformably on the Triassic Kingriali Formation and is overlain by the Middle Jurassic Samana Suk Formation (figure 3A, B). It is 136 m thick at Nammal Gorge section and 96 m at Zaluch Nala section (figures 5 and 6). Lithologically, the formation is comprised of 50% sandstone lithology. The sandstone layers are characterized by coarse- to very coarse-grained in texture, cross-bedding and having local bioturbation. It is variegated in

colour and horizontally bedded as well as cross-bedded at places. The reddish colour represents subaerial exposure and oxidation of the iron ores within sandstone lithofacies. There are also coaly clasts within sandstone lithofacies at some places (figure 3C). Conglomerate contributes less to the whole lithology of the formation and mostly occurs at the base of the formation. It is of pebbly grade and contains reworked coal patches (figure 3D). Shale covers about 30% of the lithology of the formation. The shale lithology is grey to dark black in colour, laminated, carbonaceous at places and has occasional interbeds of thin sandstones (figure 3E). The shale content increases towards top of the formation and represents fining upward sequence within the formation (figures 5 and 6). Dolomite is the third dominant lithology in the Datta Formation which is up to 10% of the whole succession. It is sandy in nature and dominated in the upper part of the formation. The coal lithofacies is bituminous in nature and occurs as coal beds in the middle part of the formation (figures 5 and 6). It also occurs in the form of coal patches within the sandstone and conglomeratic lithofacies. Pyrite

mineralization is also found in association with coal beds within the formation (figure 3F).

4.2 Organic geochemical approach

The organic geochemical attributes of Datta Formation including (i) source rock generative potential, (ii) kerogen types, (iii) indigenous nature of hydrocarbons, and (iv) thermal maturity of the organic matter are studied and described as:

4.2.1 Source rock generative potential

The TOC values of the samples of carbonaceous shales and coals of the Datta Formation from the Nammal Gorge and Zaluch Nala sections are generally $> 0.5\%$ (table 1). The minimum TOC of the samples from the Nammal Gorge section is 0.45% (DN-2), while the maximum TOC is 12.5% (DN-12), with an average of 2.96% (table 1). Likewise, the TOC values of the samples from the Zaluch Nala section range from 0.44% (DZ-16) to 8.32% (DZ-7) and have an average of 2.19% (table 1). These values suggest that the Datta Formation coals and carbonaceous shales have the potential for hydrocarbon generation as they are $>0.5\%$. However, the grey shales have TOC of $0.45\text{--}0.82\%$ and therefore have little source rock potential (e.g., Peters 1986; Hunt 1995; Khan *et al.* 2018; Ali *et al.* 2019; Hakimi *et al.* 2019, 2020).

The Rock-Eval S_1 yield for the samples from the Nammal Gorge section ranges from 0.05 (DN-27) to 4.22 mg/g (DN-12), with an average of 0.79 mg/g (table 1). For samples from Zaluch Nala, the S_1 values are negligible and indicate that migration of hydrocarbons has already occurred (Khan *et al.* 2018; Zhao *et al.* 2018).

The studied samples also show S_2 values that range from 0.48 to 78.45 mg of HC/g for the Nammal Gorge section (average: 12.93 mg/g), and from 0.20 to 70.10 mg/g (average: 14.23 mg/g) for the Zaluch Nala section (table 1). The highest S_2 yield is shown by a coal (DN-12), while the lowest values occur in the grey shales (table 1). By plotting the TOC *vs.* S_2 (Hunt 1995; Hakimi *et al.* 2018a, 2020), the source rock potential ranges from poor to excellent (table 1; figure 7A). The organic rich sediments of the Datta Formation at Nammal Gorge section had slightly better hydrocarbon generation potential than those of the Zaluch Nala section (table 1; figure 7A).

4.2.2 Kerogen types

The TOC *vs.* S_2 plot together with hydrogen index (HI) was used to determine the kerogen types in the formation (figure 7B). The plot shows that the shales and coals of the Datta Formation are dominated by Types III and II kerogen with minor Type I (figure 7B). The Type III kerogen has an HI of < 200 mg HC/g of rock, which can only generate dry gas ($C_1\text{--}C_5$) at optimum thermal maturity (Hakimi *et al.* 2014, 2018b, 2019; El-Diasty *et al.* 2017; El-Khadragy *et al.* 2018). For Type II kerogen, HI ranged from 200 to 600 mg HC/g of rock was therefore both oil- and gas-prone (Hakimi *et al.* 2014; Naeher *et al.* 2019). The minor Type I kerogen (HI > 600 mg HC/g) can act as an excellent source for liquid hydrocarbon ($>C_{6+}$) (figure 7B). The kerogens encountered within Datta Formation are mainly dominated by inertinite, vitrinite, amorphinite and minimal liptinite macerals (table 2).

4.2.3 Indigenous nature of hydrocarbons

The S_1 *vs.* TOC plot of Hunt (1995) was used to investigate the indigenous/migrated nature of the hydrocarbons present (figure 7C). Migrated hydrocarbons in general show low TOC and high S_1 values (El-Khadragy *et al.* 2018; Hakimi *et al.* 2018a). The S_1 *vs.* TOC plot indicates that the OM is indigenous and the hydrocarbons produced by the Datta Formation were, therefore, not migrated from external sources (Hunt 1995; Ding *et al.* 2013; figure 7C). Moreover, the low values of the S_1 yield compared to S_2 also suggest the indigenous nature of the hydrocarbon present (Khan *et al.* 2018; El-Khadragy *et al.* 2018; table 1).

4.2.4 Thermal maturity

T_{\max} of the samples from the Nammal Gorge section ranges from 416 to 455°C with an average of 433°C , while for samples from Zaluch Nala section, it ranges from 415 to 442°C with an average of 431°C (table 1). The average T_{\max} values of the Datta Formation samples lies within the optimum range for hydrocarbon generation (i.e., $430\text{--}470^\circ\text{C}$; Hunt 1995). Variations in thermal maturity relate to changes in kerogen type, organic composition and burial depth. A T_{\max} *vs.* HI plot indicates that coals and carbonaceous shales in the Datta Formation are thermally mature, while the grey shales are immature (figure 7D). The T_{\max} *vs.* HI plot also

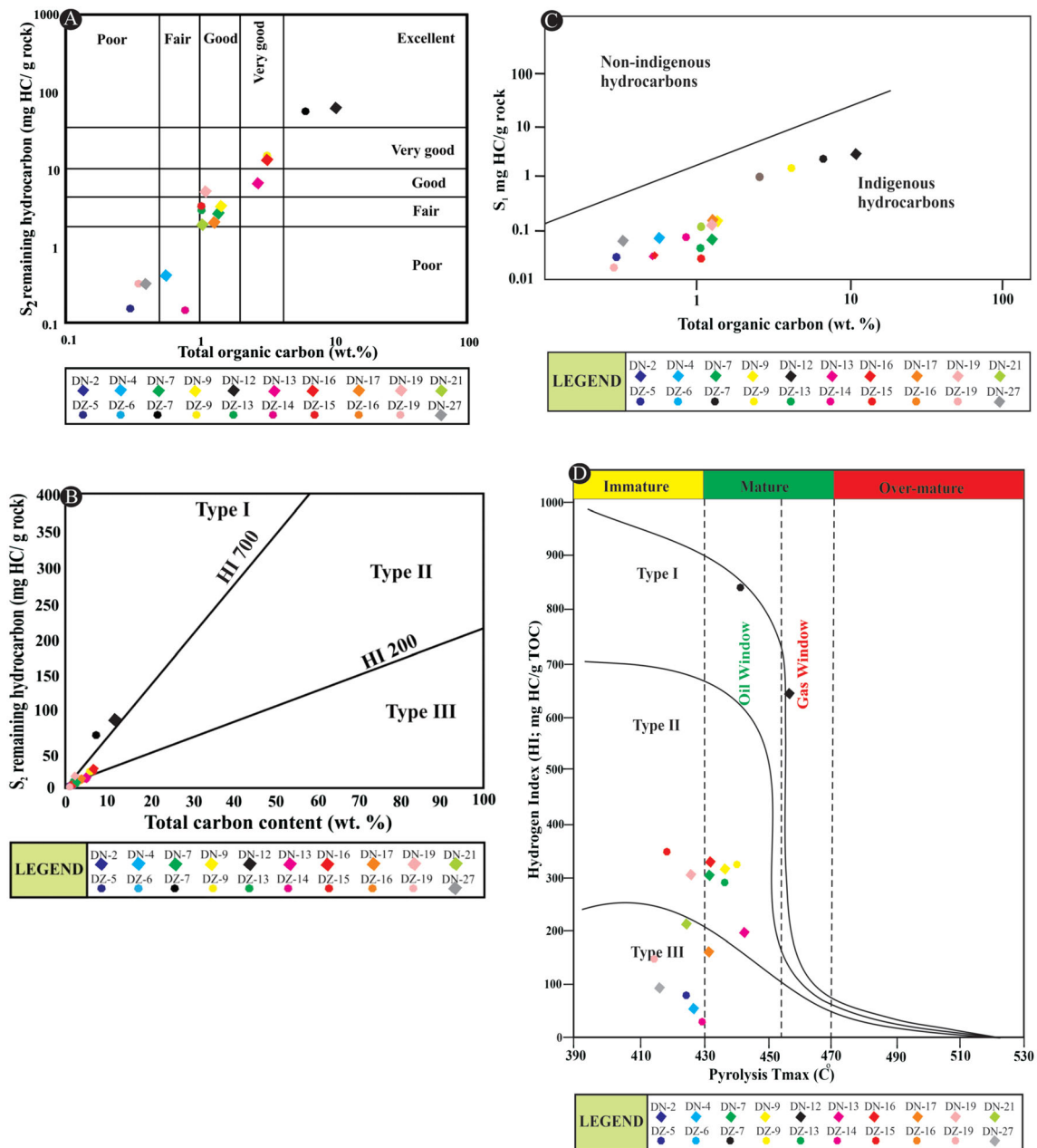


Figure 7. Plots showing distribution of organic geochemical results of the analysed samples on standard source rock diagrams. (A) TOC vs. S_2 indicating source rock types, quality of organic matter and hydrocarbon generative potential of the Datta Formation (after Peters 1986; Hunt 1995); (B) kerogen plot indicating kerogen and organic matter types encountered within the formation (after Peters 1986; Hunt 1995); (C) S_1 vs. TOC elucidating hydrocarbon types and their (non)-indigenous nature (after Hunt 1995; El-Khadragy *et al.* 2018); and (D) HI vs. T_{max} presenting kerogen types and thermal maturity levels of the analysed rock samples from Datta Formation (after van-Krevelen 1993; Hunt 1995).

indicates that Type III and II kerogens are mostly mature and lie within the oil window (Hunt 1995; Ding *et al.* 2013; Huang *et al.* 2017; Ali *et al.* 2019; figure 7D).

4.3 Palynofacies approach

Palynofacies components in the Datta Formation were classified into phytoclasts, palynomorphs and

amorphous organic matter (AOM) based on qualitative and quantitative measurements following standard classification schemes (Dow 1982; Tyson 1995; table 2).

The phytoclasts observed in the studied samples are mostly opaque but some are translucent (figure 8A–C), their macerals comprise inertinite (black phytoclasts), vitrinite (brown phytoclasts) and cutinite (yellow phytoclasts) of kerogen

Table 2.. Percentage distribution of palynofacies components including palynomorphs, phytoclasts and AOM with kerogen macerals such as inertinite, vitrinite and amorphinite for each sample at studied sections.

Palynofacies code	Sample code	Palynofacies components			Kerogen macerals		
		Palynomorphs (%)	Phytoclasts (%)	AOM (%)	Inertinite (%)	Vitrinite (%)	Amorphinite (%)
PDN-4	DN-27	15	40	45	15	25	60
	DN-21	35	40	25	16	24	60
	DN-19	20	42	38	18	24	58
Average	=	23.33	40.67	36	16.33	24.33	59.33
PDN-3	DN-17	14	44	42	24	20	56
	DN-16	10	46	44	24	22	54
	DN-13	8	52	40	26	26	48
Average	=	10.67	47.33	42	24.67	22.67	52.67
PDN-2	DN-12	5	79	16	30	49	21
PDN-1	DN-9	17	44	41	20	24	58
	DN-7	15	48	37	23	25	52
	DN-4	12	53	35	23	30	47
	DN-2	10	65	25	28	36	36
Average	=	13.5	52.5	34.5	24	28.5	48
PDZ-4	DZ-19	10	70	20	20	50	30
	DZ-16	0	0	0	0	0	0
	DZ-15	2	90	8	68	22	10
Average	=	6	80	14	44	36	20
PDZ-3	DZ-14	1	93	6	70	23	7
	DZ-13	6	84	10	72	12	16
	DZ-9	2	95	3	45	50	5
Average	=	3	90.67	6.33	62.33	28.33	9.33
PDZ-2	DZ-7	1	97	2	46	51	3
PDZ-1	DZ-6	0	0	0	0	0	0
	DZ-5	1	89	10	65	24	11
Average	=	1	89	10	65	24	11

macerals following the guidelines of Ercegovac and Kostic (2006), Filho *et al.* (2012) and Khan *et al.* (2018). Opaque/black phytoclasts include Type III kerogen macerals and are responsible only for dry gas generation upon thermal maturation (Tyson 1995; Zoba *et al.* 2013; Ali *et al.* 2019; figure 8A). The translucent phytoclasts include Type II kerogen macerals and can generate wet gas when optimum thermal maturity is reached (Dow 1982; Traverse 2007; Khan *et al.* 2018; figure 8B, C). Palynomorphs are in general, lipid rich, prone to high capability of oil generation. They include Type I kerogen macerals as shown in figure 8(D–F) (Jiang *et al.* 2008; El-Diasty *et al.* 2017; Ali *et al.* 2019). The AOM encountered within the studied samples is granular as well as gelified in nature. It is considered to be potentially responsible for liquid hydrocarbon generation, provided that optimal

thermal maturity is attained (Tyson 1995; Pacton *et al.* 2011; Schneider *et al.* 2019; figure 8G–I). The terms amorphinite and AOM are used interchangeably for the sake of kerogen classification and are included in Type I kerogen macerals (Tyson 1995; Pacton *et al.* 2011). The palynofacies types inferred from the samples of the Datta Formation are categorized on the basis of their maceral types, morphology, abundance and distribution on ternary kerogen plots of Dow (1982) and Tyson (1995). By studying the sections from the Nammal Gorge and Zaluch Nala sections, we have recognized eight palynofacies assemblages, four for each section (i.e., PDN-1 to PDN-4 for Nammal Gorge section and PDZ1–PDZ4 for the Zaluch Nala section). Description of the Nammal Gorge and Zaluch Nala palynofacies and their interpretations are summarized as:

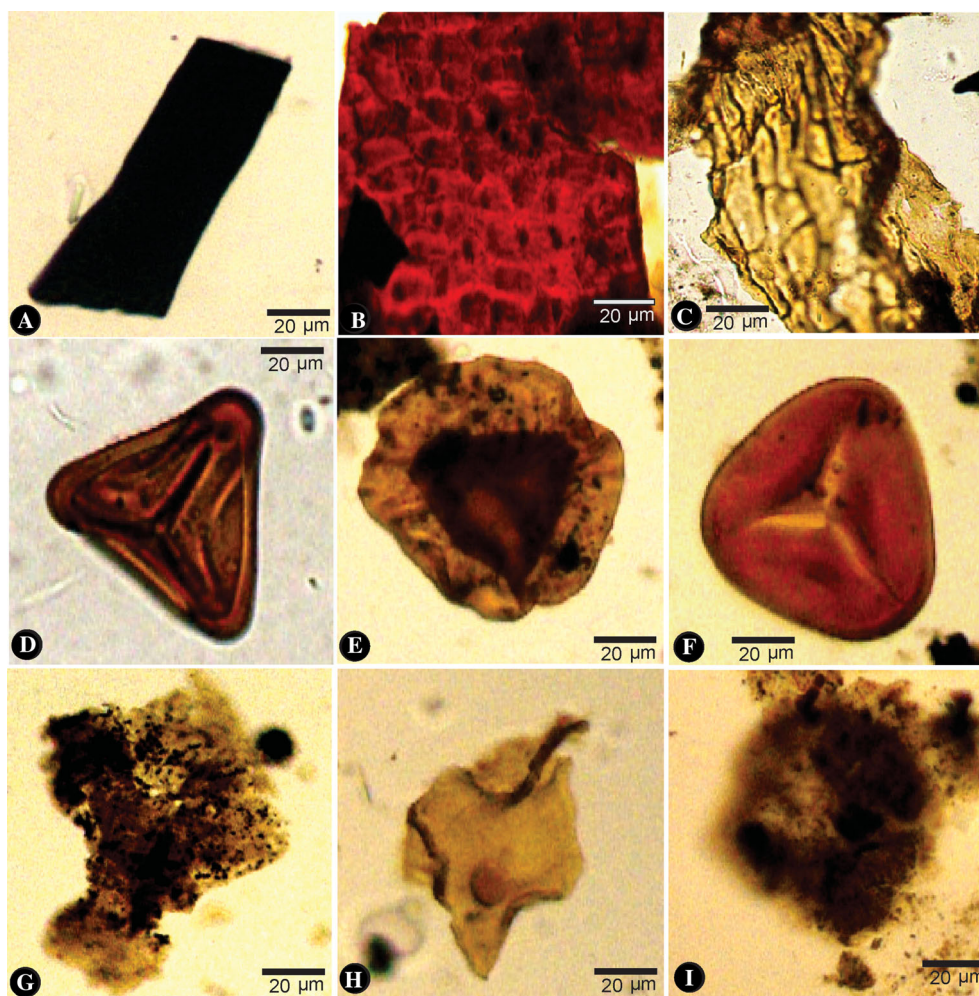


Figure 8. Palynofacies components including phytoclasts, palynomorphs and AOM identified within Datta Formation at Nammal and Zaluch Nala sections, Potwar Basin. (A) Opaque phytoclast/inertinite, the black colour reflects over thermal maturity or oxidation of the organic matter. These phytoclasts are thermally inert or can only generate dry gas (Dow 1982; Tyson 1995; Khan *et al.* 2018). (B and C) Bio-structured (translucent) phytoclasts with original trigonal and tetragonal cellular arrangement derived from terrestrial plants. Such phytoclasts are considered as vitrinite macerals and are responsible for wet gas generation on achievement of optimum thermal maturity (Tyson 1995; Khan *et al.* 2018). (D, E and F) Trilobate–trilete spore, monosaccate pollen and trilete spore, respectively, of higher plants. These macerals are responsible for liquid hydrocarbon generation and constitute liptinite components of the kerogen macerals (Jiang *et al.* 2008; Khan *et al.* 2018). (G, H and I) Dark brown granular AOM of marine origin, light brown gelified AOM of terrestrial origin and thermally cooked AOM, respectively. These macerals are prone to liquid hydrocarbon generation and constitute amorphinite components of the kerogen macerals (Khan *et al.* 2018).

4.3.1 The Nammal Gorge section

4.3.1.1 *PDN-1*: Palynofacies PDN-1 is identified in samples DN-2, DN-4, DN-7 and DN-9 from the lower part of the formation (figure 5; table 2), and contains 24% inertinite, 29% vitrinite and 48% amorphinite and liptinite (figure 9A, B; table 2). The first two components are well-preserved and display an equi-dimensional morphology suggesting long-distance transport from source area (Tyson 1995; Ali *et al.* 2019; figure 9A, B). The amorphinite/AOM is dark brown to light brown in

colour and gelified in nature suggesting a terrigenous origin (Pacton *et al.* 2011; Ghasemi-Nejad *et al.* 2009; figure 9A, B). The liptinite macerals include trilete spores and monosaccate pollen which are yellowish to brown under transmitted light (figure 9B). Palynofacies assemblage PDN-1 falls within the wet gas and condensate zone of Dow (1982) on a liptinite–vitrinite–inertinite (LVI) ternary kerogen plot for which kerogen Type II has been suggested (Dow 1982; figure 10). The palynofacies represents a shelf to basin transition with anoxic conditions (Tyson 1995; figure 11) and the

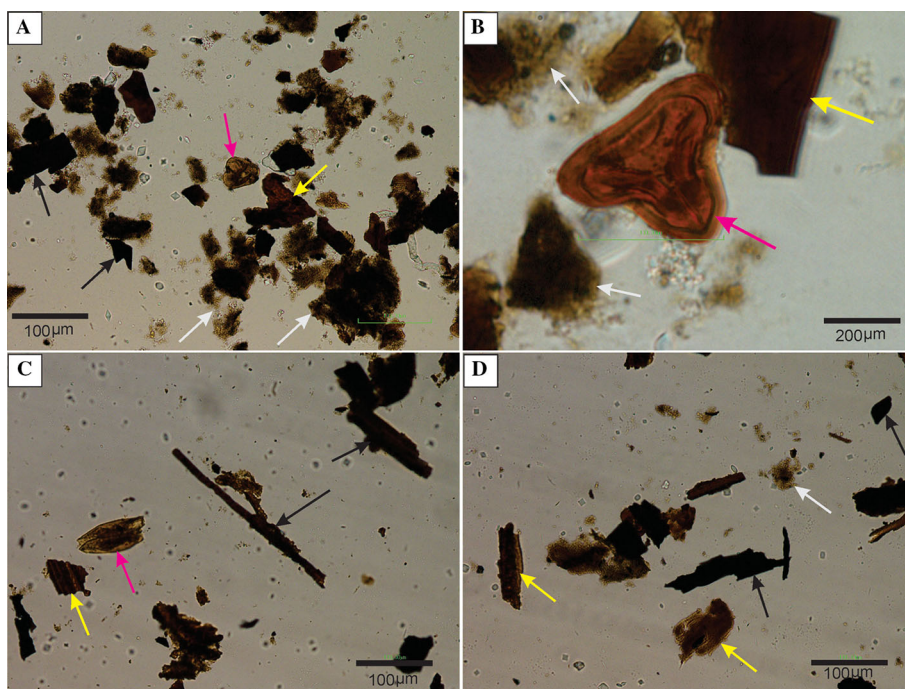


Figure 9. Photomicrographs of palynofacies PDN-1 and PDN-2 of Datta Formation at the Nammal Gorge section. (A) Dry gas-prone opaque phytoclasts/inertinite (black arrows), oil prone palynomorphs/liptinite (pink arrow), oil prone gelified AOM (white arrows), and wet gas-prone brown phytoclasts/vitrinite (yellow arrow) in transmitted light in PDN-1; (B) vitrinite (yellow arrow), trilete spore (*Trilobosporites laevigatus*; pink arrow) and oil prone gelified AOM (white arrows) in PDN-1; (C) elongated opaque phytoclasts/inertinites (black arrows), vitrinite (yellow arrow) and *Matonisporites crassiangulatus* sp. (spore; pink arrow) in dry gas-prone PDN-2 palynofacies; and (D) vitrinite (yellow arrows), elongated inertinite (black arrows), and granular AOM/amorphinite (white arrow) faced in PDN-2 at the Nammal Gorge section.

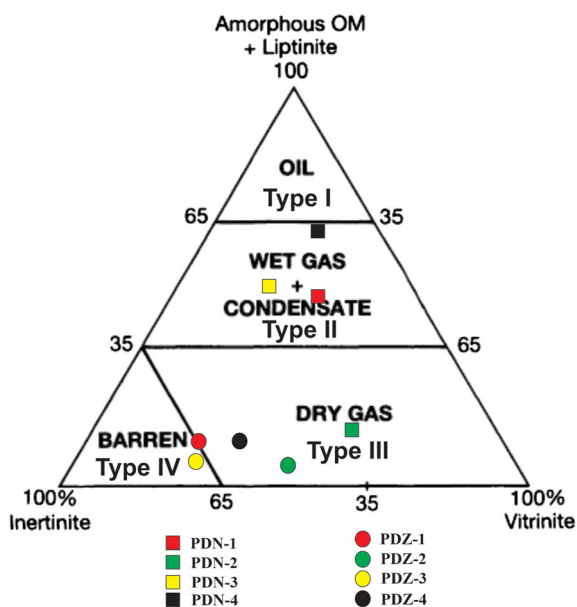


Figure 10. Liptinite–vitrinite–inertinite (LVI) ternary kero-gen plot with fields indicating expected hydrocarbons for palynofacies of Datta Formation at Nammal Gorge and Zaluch Nala sections.

prevalence of anoxic conditions is indicated by the presence of AOM (Naehler *et al.* 2019; Schneider *et al.* 2019).

4.3.1.2 *PDN-2*: Palynofacies assemblage PDN-2 is recognized from a 1.5-m thick coal bed (DN-12) at the Nammal Gorge section (figure 5). It consists of 30% inertinite, 49% vitrinite, 21% amorphinite and liptinite (figure 9C, D; table 2). The maceral morphology (based on elongated shapes and sharp outlines) of the inertinite and vitrinite suggested limited transportation from the source area and derivation from higher terrestrial plants (Tyson 1995). The dominance of inertinite and vitrinite over liptinite and amorphinite together indicate the dry gas-prone nature of this palynofacies (Khan *et al.* 2018; Schneider *et al.* 2019). On a ternary plot, Type III kerogen is suggested (figure 10; table 2), and PDN-2 represents a marginal dysoxic–anoxic shelf setting on a Tyson’s (1995) ternary kerogen plot (figure 11). The dysoxic and anoxic conditions support the organic matter preservation within this palynofacies (Naehler *et al.* 2019). This palynofacies represents a good source rock at the Nammal Gorge section in accordance to TOC and Rock-Eval results (table 1).

4.3.1.3 *PDN-3*: Palynofacies assemblage PDN-3 has been encountered within samples DN-13,

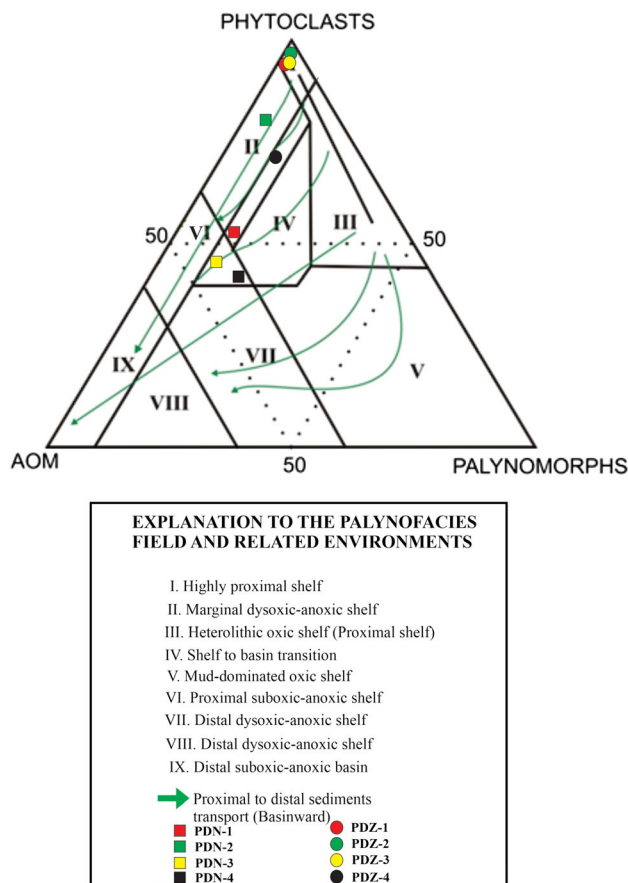


Figure 11. AOM–phytoclast–palynomorph (APP) ternary plot showing percentage distribution of identified palynofacies and their depositional environments at studied sections.

DN-16 and DN-17. It includes 25% inertinite, 23% vitrinite and 52% amorphinite and liptinite (figure 5; table 2). Based on the ternary plots of Dow (1982) and Tyson (1995), the assemblage contains oil and gas-prone Type II kerogen (figures 10 and 11). The amorphinite and liptinite are prone to liquid hydrocarbon generation at optimum thermal maturity (Khan *et al.* 2018; Ali *et al.* 2019). Thus, the high proportion amorphinite and liptinite causes the palynofacies to be oil prone; however, the substantial amount of inertinite and vitrinite gives it some wet gas generating potential (figure 12A, B; Zoba *et al.* 2013; Schneider *et al.* 2019). This palynofacies represents a shelf to basin transition zone on Tyson (1995) kerogen plot in close proximity to proximal suboxic to anoxic shelf settings (figure 11).

4.3.1.4 *PDN-4*: Palynofacies assemblage PDN-4 is from samples DN-19, DN-21 and DN-27 which are collected from the upper part of the Datta Formation at the Nammal Gorge section. This

palynofacies is characterized by inertinite (16%), vitrinite (24%), liptinite and amorphinite (60%; figure 5; table 2). Vitrinite and inertinite are comparatively low in abundance, but are well preserved and show regular biostructured cellular nature which indicates a dominance of anoxic marine depositional conditions (Ghasemi-Nejad *et al.* 2009; Naeher *et al.* 2019). The yellow colour of the liptinite macerals indicates that PDN-4 is rich in lipids and thus, can generate liquid hydrocarbons once the kerogen attains maturity conditions (Zoba *et al.* 2013; El-Diasty *et al.* 2017). The abundance of amorphinite and liptinite (60%) shows oil prone kerogen Type I but on a Dow (1982) LVI ternary plot, this palynofacies lies in the zone of Type II kerogen and hence can generate both oil and gas (figure 10). It plots within the shelf to basin transition zone on a Tyson (1995) APP kerogen plot (figure 11).

4.3.2 The Zaluch Nala section

4.3.2.1 *PDZ-1*: Palynofacies PDZ-1 is present within samples DZ-5 and DZ-6 (figure 6). This palynofacies is dominated by kerogen macerals including 65% inertinite, 24% vitrinite, and 11% liptinite and amorphinite (table 2). The inertinite and vitrinite are equi-dimensional and some are lath-shaped (figure 12A, B). Inertinite is dominant over vitrinite, liptinite and amorphinite, which reflects susceptibility to dry gas generation (Dow 1982; Tyson 1995; Ghasemi-Nejad *et al.* 2009). The vitrinite components appear translucent in transmitted light and are prone to wet gas generation upon thermal maturation (Koch *et al.* 2017). The amorphinite is entirely granular, thermally cooked and insignificant in quantity. Generally, the palynomorphs are prone to oil generation in sedimentary basins (Traverse 2007); however, their poor preservation leads to its insignificance in PDZ-1 (figure 12B). On Dow (1982) LVI kerogen plot, PDZ-1 falls in-between the dry gas zone and the inert zone (figure 10). On Tyson (1995) ternary kerogen plot, it plots within a highly proximal shelf setting (figure 11) for which a dry gas prone Type III kerogen is suggested (Tyson 1995; Hakimi *et al.* 2014). The abundance of inertinite and its black colour also support highly proximal shelf setting for its deposition (El-Diasty *et al.* 2017; Schneider *et al.* 2019).

4.3.2.2 *PDZ-2*: This palynofacies is observed in samples DZ-7 acquired from coal bed at Zaluch

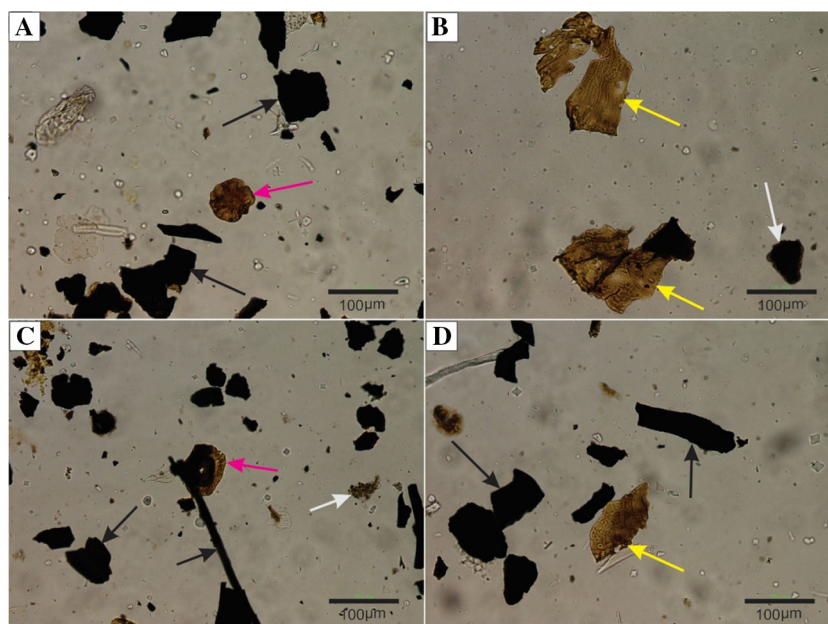


Figure 12. Dry gas-prone palynofacies PDZ-1 (A–B) and wet gas and condensate prone palynofacies PDZ-3 (C–D) from Zaluch Nala section in transmitted light. (A) Dry gas-prone equidimensional opaque phytoclasts (black arrows) and oil prone palynomorph (pink arrow); (B) wet gas-prone light brown phytoclasts with original curved rectangular cellular structures (yellow arrows) and thermally cooked AOM (white arrow); (C) inertinite (black arrows), monosaccate pollen (pink arrow) and granular AOM (white arrow); and (D) vitrinite (yellow arrow) with fibrous cellular structures and oxidized inertinite (black arrow).

Nala section (figure 6). This palynofacies is dominated by kerogen macerals, i.e., 46% inertinite, 51% vitrinite and 3% liptinite and amorphinite (table 2). The first two are well-preserved and appear dark black and brown in transmitted light, respectively (figure 12C, D). The inertinite is dominant over liptinite and amorphinite which showed low potential for liquid hydrocarbon (Zhang *et al.* 2015). Moreover, inertinite in this palynofacies is mostly over-cooked which can generate only dry gas (Zoba *et al.* 2013; Koch *et al.* 2017). The palynomorphs are also thermally cooked and thus are overmature according to the spore colour index (SCI) and thermal alteration index (TAI). AOM counts for a very low quantity and is thermally cooked in this palynofacies. On Dow (1982) LVI ternary kerogen plot, this palynofacies plots within the dry gas zone and hence reflects kerogen Type III (figure 10). This palynofacies is deposited in a highly proximal shelf (i.e., zone I) on Tyson (1995) APP ternary kerogen plot (figure 11) and hence represents according to Tyson (1995) a dry gas-prone Type III kerogen.

4.3.2.3 *PDZ-3*: The palynofacies PDZ-3 is represented by samples DZ-9, DZ-13 and DZ-14 collected from carbonaceous shales at Zaluch Nala

section (figure 6). It is dominated by kerogen macerals including 62% inertinite, 28% vitrinite, and 9% liptinite and amorphinite (table 2). Most of the inertinites within this palynofacies are biodegraded and oxidized that represents less potential for hydrocarbons. The oxidized inertinites are opaque in transmitted light and show inertness for hydrocarbon generation. On a Dow (1982) LVI ternary plot, this palynofacies lies within the barren zone having Type III/IV kerogen (figure 10), while on Tyson (1995) kerogen, it falls within the proximal shelf zone which also supports its inert kerogen types (figure 11). In the current study, this facies is regarded as barren palynofacies from hydrocarbon source point of view as it is lying in inert/barren zone on Dow (1982) kerogen plot and can seldom generate any hydrocarbons except some dry gas (Hakimi *et al.* 2014; Koch *et al.* 2017).

4.3.2.4 *PDZ-4*: This palynofacies is documented in samples (DZ-15, DZ-16, DZ-19) collected from upper part of the formation (figure 6). It is dominated by kerogen macerals including 44% inertinite, 36% vitrinite, and 20% liptinite and amorphinite (figure 13A–D). On Dow (1982) LVI ternary kerogen plot, PDZ-4 palynofacies lies within the dry gas zone suggesting gas prone Type

III kerogen (figure 10). On Tyson (1995) APP ternary kerogen plot, this palynofacies falls within shelf to basin transition zone (i.e., zone IV) having anoxic conditions (figure 11). Sufficient amount of palynomorphs/liptinite are also present in this palynofacies which dominantly included alete spores and monosaccate pollen along with fungal hyphae that constitute kerogen components. The prevalence of anoxic conditions during its deposition supports the preservation of palynomorphs and fungal hyphae within this palynofacies (Traverse 2007; Zhang *et al.* 2015).

4.4 Visual thermal maturation via SCI/TAI

With regard to estimating visual thermal maturity, the colour of three specific palynomorphs species (*Deltoideospora* sp., *Classopollis torosus* sp. and *Trilobosporites laevigatus* sp.) were used and compared with Spore Colour Index (SCI) and Thermal Alteration Index (TAI) standard charts. The PDN-1 palynofacies shows an orange brown colour on SCI and TAI colour charts, which is equivalent to a numeric thermal maturity of 7 on SCI and 3 on TAI. This indicates that the palynofacies is thermally mature and corresponds to the main phase of wet gas generation. In PDN-2, palynomorphs are consistently dark brown with a value of 8 on SCI and 3+ on TAI, also indicating

thermally mature conditions. However, it is gas-prone and corresponds to the dry gas window. PDN-3 palynomorphs are yellow to orange in colour with a thermal maturity of 5 and 2+ on SCI and TAI charts, respectively. These values suggest a range of immature to mature oil/gas zone maturity. PDN-4 is thermally immature as its palynomorphs are lemon yellow in colour and have numeric maturity values of 3 on SCI and 2+ on TAI and cannot generate hydrocarbons (El-Diasty *et al.* 2017).

The PDZ-1 thermal maturity is 7 on SCI and 3 on TAI and shows mature zone of the main phase of wet gas generation (Pross *et al.* 2007; Koch *et al.* 2017; Ali *et al.* 2019). The thermal maturity of PDZ-2 is 10 on SCI and 4 on TAI which indicates that it is thermally 'well-cooked' beyond the oil window and can produce only dry gas. Here, SCI and TAI slightly differ from the geochemical results which revealed that PDZ-2 is thermally mature; however, based on SCI characteristics, it is an overmature palynofacies. This dark black colour and contrast with geochemical results may be due to oxidation of the palynomorphs during maceration process or surface weathering at outcrop (Tyson 1995; Naeher *et al.* 2019). PDZ-3 is characterized by lemon brown palynomorphs and on SCI its thermal maturity is 7, while on TAI is 3 and hence can act as mature

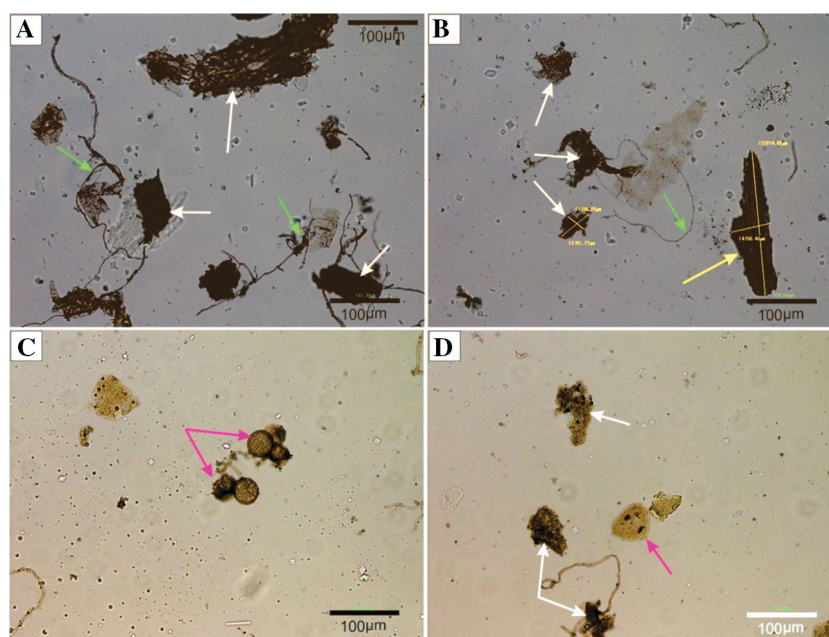


Figure 13. Oil and gas-prone PDZ-4 palynofacies encountered within Datta Formation at the Zaluch Nala section. (A) Thermally cooked AOM (white arrows), fungal hyphae and filaments (green arrows); (B) biostructured phytoclasts (yellow arrows), gelified AOM (white arrows), fungal hyphae (green arrow); (C) fungal spores (pink arrows) in transmitted light; and (D) granular AOM (white arrows) and spore (pink arrow).

palynofacies prone to gas generation. On SCI and TAI, PDZ-4 thermal maturity is 3 and 2, respectively. Thus, PDZ-4 is thermally immature to generate hydrocarbons (Koch *et al.* 2017). Overall, the SCI and TAI investigations revealed that the Datta Formation possess both mature and immature source rock intervals with no obvious overmature beds, and palynofacies investigations are consistent with the geochemical results.

5. Discussion

5.1 Origin and preservation of the organic matter

Organic input of the Datta Formation is dominated by phytoclasts and AOM with a minor contribution of palynomorphs (figure 8A–F; table 2). Phytoclasts are mainly derived from terrigenous sources, i.e., gymnosperms that survived on Indian Plate during Early Jurassic (Kuerschner *et al.* 2017; Ali *et al.* 2019). The palynomorphs including Jurassic pollen and spore are resultant from higher terrestrial plants (figure 8D–F). The AOM encountered within Datta Formation is entirely granular and seems to be derived from marine phytoplankton, degraded phytoclasts, fungal tissues, bacteria and algae (Tyson 1995; El-Diasty *et al.* 2017). However, a minor AOM content is gelified in nature and seems to be possibly derived from higher plant cuticles (Ercegovac and Kostic 2006; Traverse 2007; Pacton *et al.* 2011; figure 8G–J). The overall, palynofacies considerations suggest that the OM is mostly terrigenous in origin with an episodic influx of marine OM. The variation in OM types suggests fluctuations in preservation conditions. The abundance of Type III kerogen within organic rich shale and coal intervals of Datta Formation also elucidate the derivation of organic matter from terrestrial sources (Traverse 2007; Koch *et al.* 2017). The palynofacies investigation shows that oxygen deficient suboxic to anoxic conditions prevailed during deposition of the Datta Formation. These anoxic conditions enhanced the preservation of OM as evidenced by dark grey to black colour of the shale and coal intervals (Tyson 1995; Naeher *et al.* 2019). The anoxic conditions are also witnessed by the presence of pyrite in coal and organic rich shale beds (El-Atfy *et al.* 2016; Schneider *et al.* 2019).

5.2 Palaeo-depositional environment

The Datta Formation is characterized by a range of lithofacies including conglomerates, sandstones, shales, dolomites and coals (Abbasi *et al.* 2012; Iqbal *et al.* 2015, 2019; figures 5, 6 and 14). The conglomerates and sandstones are interpreted to represent deposition in a fluvial environment (channel), while the organic-rich shales and dolomite represent deposition in near-shore lagoonal and swamp environments that support organic matter accumulation and preservation (Abbasi *et al.* 2012; Iqbal *et al.* 2015; figure 14). The conglomerate is clast-supported and represents channel lag deposits. The basal conglomerate also possesses erosive surfaces and laterites that indicate regional sea level fall and consequently erosion (Iqbal *et al.* 2015). The coaly clasts within conglomerate and sandstone lithofacies show erosion and reworking of the nearby pre-existing coal deposits (Kadri 1995; Iqbal *et al.* 2019). The coal beds and coaly clasts show prevalence of hot humid palaeoclimate during its deposition. The sea level fall is also supported by ocanoclasts/phystocalsts influx into the system from terrestrial environments. The coal beds show deposition in water saturated, swampy settings with abundant terrigenous OM (Tyson 1995; Abbasi *et al.* 2012; figure 14). TOC-rich beds (coal beds) in the Datta Formation are best explained by both high primary productivity and establishment of prolonged phases of anoxic conditions in a near-shore, fluvio-deltaic depositional environment (El-Atfy *et al.* 2016; Naeher *et al.* 2019). Furthermore, the enrichment of OM, mostly by Type III kerogen within Datta Formation, shows its deposition in a fluvio-deltaic setting influence by both riverine and marine processes. Episodic marine incursions were accompanied by relatively oxygen-deficient conditions that resulted into preservation of phytoclasts, palynomorphs and AOM (Koch *et al.* 2017; Naeher *et al.* 2019). Opaque phytoclasts in the Datta Formation indicate oxidizing settings and exposure to subaerial conditions that affect OM preservation (Tyson 1995; Naeher *et al.* 2019). Woody fragments/coal patches, phytoclasts and terrigenous palynomorphs indicate the continental origin of the OM (Tyson 1995; El-Atfy *et al.* 2016).

5.3 Palaeo-geography and regional comparison

The lithofacies and palynofacies patterns observed in this study and those available in published

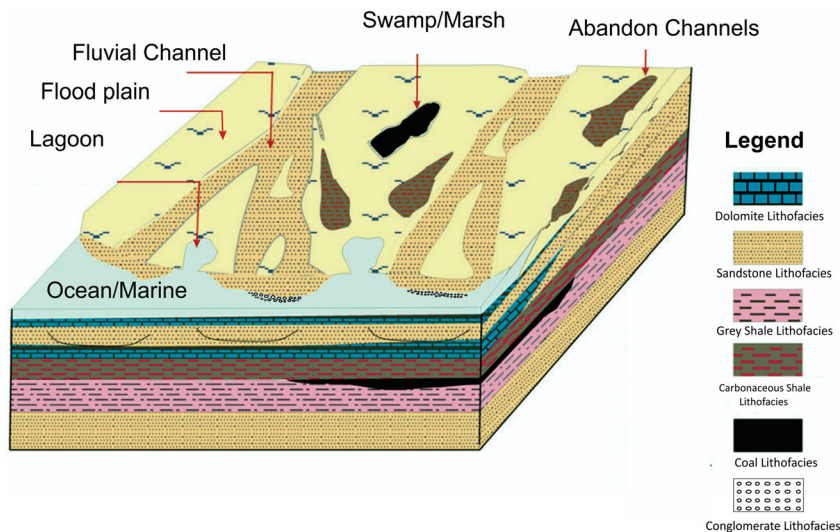


Figure 14. Palaeo-depositional model illustrating the distribution of various lithofacies encountered within Datta Formation and their sub-depositional environments (after Abbasi *et al.* 2012).

literature allow a tentative comparison between Lower Jurassic sediments (Datta Formation) in the Potwar Basin of Pakistan and coeval Lathi Formation in the Jaisalmer Basin of India (figure 4A, B). Palaeo-geographically, both basins were located on the northwestern passive margin of the Indian Plate during Early Jurassic Period and the sedimentary successions were deposited at the margin of Neo-Tethys Ocean under similar depositional, biogeochemical and geomorphological conditions (Kazmi and Jan 1997; Craig *et al.* 2018; Iqbal *et al.* 2019; figure 4B). Organic geochemically, both Datta and Lathi formations contain dominantly Types II and III kerogens with good to excellent source rock potential and of similar provenance (Rai *et al.* 2016; Pandey *et al.* 2019). Phytoclasts and palynomorphs derived from similar sources (i.e., continental gymnosperm) have been encountered in both stratigraphic units (Rai *et al.* 2016; Kuerschner *et al.* 2017). Likewise, both current and previous studies on the Datta Formation and on Lathi Formation (e.g., Abbasi *et al.* 2012; Pandey *et al.* 2012; Zadan and Arbab 2015; Iqbal *et al.* 2015, 2019; Rai *et al.* 2016; Pandey *et al.* 2019) show the presence of similar lithologies including conglomerates, sandstones, shales and coals that were deposited under similar conditions in the two basins. The reworked coal patches (woody fragments) encountered in conglomeratic lithofacies of Datta Formation (figure 3D) are exactly similar to that of Lathi Formation; they represent derivation from similar sources during Early Jurassic time (Pandy *et al.* 2012). The coal beds (marker horizons) encountered in both

formations are bituminous and possess similar maceral compositions (Zadan and Arbab 2015). Overall, the Datta Formation was deposited in a fluvio-deltaic setting with episodic suboxic to anoxic marine conditions and this is consistent with other Lower Jurassic Gondwanian sediments including the Lathi Formation (figure 14). Furthermore, both the Datta and Lathi formations possess a regional unconformity characterized by conglomeratic beds and erosive surfaces at their bases that represents regional sea level fall during Early Jurassic (Iqbal *et al.* 2015, 2019; Zadan and Arbab 2015; Rai *et al.* 2016). This regional seal level drop shows the subaerial exposure and oxidation of sediments (laterites) in Neo-Tethys realm that has been found within the basal parts of both of the formations. Moreover, an Early Jurassic (Hettangian) age has been assigned to both units on the basis of their palynological and palynofacies characteristics that further strengthen the regional comparison between the two formations (Pandy *et al.* 2012; Zadan and Arbab 2015; Kuerschner *et al.* 2017). Abundant *Classobollis*, *Spheripollenites*, *Gliscopollis*, *Inaperturopollenites* and *Araucariacites* species and lack of diagnostic Late Triassic and Middle Jurassic sporomorphs suggested Early Jurassic age for the Lathi Formation (Pandy *et al.* 2012).

Palaeo-climatic signatures may also affect basin architecture and consequently affect sediment characteristics at regional scale (Mertmann 2003). Palaeo-climatic signatures such as, laterites, fire-clay, paleosols and bioturbation encountered within the Datta and Lathi formations indicate a

warm-humid, tropical to sub-tropical climate on the northwestern margin of the Indian Plate during Early Jurassic time. These signatures represent a substantial increase in precipitation, humidity and vegetation cover along the NW margin of the Indian Plate (Iqbal *et al.* 2015; Kuerschner *et al.* 2017). The hot-humid climate most likely allowed the transportation of continent-derived OM along with sediments brought by high rainfall and frequent freshwater flow into the Potwar and Jaisalmer basins during the Early Jurassic Period (Rai *et al.* 2016). Thus, the Lower Jurassic strata of Potwar and Jaisalmer basins possess striking similarities in terms of lithology, sequence stratigraphy, fossil records, sediment provenance, OM content and source rock potential across the basins (e.g., Mertmann 2003; Iqbal *et al.* 2015; Craig *et al.* 2018; Pandey *et al.* 2019).

6. Conclusions

A combined lithostratigraphic, bulk organic geochemical and palynofacies investigations focusing on the Lower Jurassic Datta Formation in the western Salt Range (Potwar Basin, Pakistan) allowed to draw the following conclusive remarks:

- The formation is dominated by sandstone (50%), shale (30%), conglomerate (10%), dolomite (5%) and coal lithofacies (5%). The organic rich lithologies such as coal and shale were studied to assess their source rock potential and organic matter types.
- The coals and shales of the Datta Formation are dominated by Type III and Type II kerogens with minor Type I kerogen. The maturity level of these kerogens ranges from thermally immature to mature with no obvious over-matured conditions. The variation in thermal maturity of the OM is due to change in the kerogen types as well as due to change in burial depth.
- The organic geochemical results showed that the shales and coals in the Datta Formation contain sufficient OM (0.5–12.50 wt.% TOC) to act as potential source rocks for hydrocarbon generation. Some beds represent excellent source rock potential (e.g., the coal intervals) for hydrocarbon generation. Others (e.g., carbonaceous shales) reflect good-to-very good source rock characteristics and some layers (e.g., grey shales) exhibited poor-to-moderate source rock quality.
- Based on relative abundance and morphology of palynofacies components, eight distinct palynofacies were identified within the formation (i.e., PDN-1 to 4 and PDZ-1 to 4). PDN-1 and PDN-4 have Type II kerogens which are prone to oil/gas generation. PDN-2 and PDN-3 have Type III kerogens and are thus prone to dry gas generation. Likewise, PDZ-1, PDZ-2 and PDZ-3 have dry gas prone Type III kerogens, whereas PDZ-4 has oil/gas prone Type II kerogen.
- Palynofacies analysis supports the bulk organic geochemical analysis and mostly reveals Type III and Type II kerogen within the formation. The kerogens encountered are mainly comprised of inertinite, vitrinite, liptinite and amorphinite, which contribute to the hydrocarbon generation potential of the formation. These kerogen types derived mainly from terrestrial sources with minor marine contributions.
- Palynomorph species such as *Deltoidospora* sp., *Classopollis torosus* sp., and *Trilobosporites Laevigatus* sp. are identified and used for visual thermal maturity estimation. The thermal maturity values of the OM vary from 3 to 10 on SCI and 2 to 4 TAI. These values are in close agreement with the bulk organic geochemical results from the studied samples of the Datta Formation.
- The organic rich sediments of the Datta Formation testify deposition in a suboxic to anoxic, nearshore fluvio-deltaic depositional environment that received predominantly terrestrial OM with subordinate marine OM influx.
- The Lower Jurassic Datta Formation in the Potwar Basin is similar to the stratigraphically equivalent Lathi Formation in the Jaisalmer Basin (NW India) in terms of lithologies, OM types and palaeo-depositional environment. Both formations were deposited on the NW margin of the Indian Plate affected by Neo-Tethys sedimentations.

Acknowledgements

National Centre of Excellence in Geology (NCEG), University of Peshawar (UOP) is acknowledged for providing facilities and finances for carrying out this research work. The National Research Program for Universities Project (No. 7939) awarded to Dr Irfan U Jan, Associate Professor at the NCEG, UOP is acknowledged for supporting this study. The authors are grateful to the two

unknown reviewers whose valuable comments and suggestions that significantly improved the quality of the manuscript.

Author statement

Nasar Khan: Main idea, conceptualization, methodology, results, interpretation and initial manuscript preparation. Irfan Ullah Jan: Supervision and validation of the results interpretation. Shahid Iqbal: Co-supervision, discussion and refinement of the manuscript. Rudy Swennen: Review, improvement of technical writing and scientific input. Osman Salad Hersi: Proof reading and technical review. Hafiz Shahid Hussain: Assistance during palynofacies analysis and general draft formatting.

References

- Abbasi I A, Haneef M, Obaid S, Daud F and Qureshi A W 2012 Mesozoic deltaic system along the western margin of the Indian Plate: Lithofacies and depositional setting of Datta Formation, North Pakistan; *Arab. J. Geosci.* **5**(3) 471–480.
- Ahmad Jr S, Ahmad Sr S, Waheed K and Ali A 2013 Facies analysis and dynamic depositional modeling: Implications for hydrocarbon prospecting in the Lower Jurassic Datta Formation, Salt Range, northwest Pakistan; *Pak. J. Hydrocarb. Res.* **23** 63–71.
- Ahmed W and Alam S 2007 Organic geochemistry and source rock characteristics of Salt Range Formation, Potwar Basin Pakistan; *Pak. J. Hydrocarb. Res.* **17** 37–59.
- Ali J R and Aitchison J C 2008 Gondwana to Asia: Plate tectonics, paleogeography and the biological connectivity of the Indian sub-continent from the Middle Jurassic through latest Eocene (166–35 Ma); *Earth-Sci. Rev.* **88**(3–4) 145–166.
- Ali F, Qiang J, Ahmad S, Khan S, Hanif M and Jan I U 2019 Sedimentological and geochemical analysis of the Middle Jurassic Shinawari Formation, Upper Indus Basin, Pakistan: Implications for palaeoenvironmental and hydrocarbon assessment; *Arab. J. Sci. Engr.* **44**(7) 6465–6487.
- Ashraf M, Ahmad M and Faruqi F A 1976 Jurassic bauxite and kaolinite deposits of Chhoi area Kala Chitta Range, Punjab Pakistan; *Geol. Bull. Punjab Univ.* **41** 41–54.
- Asif M and Fazeelat T 2012 Petroleum geochemistry of the Potwar Basin Pakistan II: Oil classification based on heterocyclic and polycyclic aromatic hydrocarbons; *Appl. Geochem.* **27**(8) 1655–1665.
- Asif M, Fazeelat T and Jalees M I 2014 Biomarker and stable carbon isotopic study of Eocene sediments of North-Western Potwar Basin, Pakistan; *J. Petrol. Sci. Eng.* **122** 729–740.
- Baker D M, Lillie R J, Yeats R S, Johnson Gd, Yousuf M and Zamin A S H 1988 Development of the Himalayan frontal thrust zone: Salt Range, Pakistan; *Geology* **16** 3–7.
- Béhar F, Beaumont V, De B and Penteado H L 2001 Rock-Eval 6 technology: Performances and developments; *Oil Gas Sci. Technol.* **56** 111–134.
- Craig J, Hakhoo N, Bhat G M, Hafiz M, Khan M R, Misra R, Sk Pandita, Aina B K, Thurow J, Thusu B, Ahmed W and Khullar S 2018 Petroleum systems and hydrocarbon potential of the north-west Himalaya of India and Pakistan; *Earth-Sci. Rev.* **187** 109–185.
- Ding W, Wan H, Zhang Y and Han G 2013 Characteristics of the Middle Jurassic marine source rocks and prediction of favorable source rock kitchens in the Qiangtang Basin of Tibet; *J. Asian Earth Sci.* **66** 63–72.
- Dow W G 1982 Kerogen maturity and type by reflected light microscopy applied to petroleum exploration; In: *Soc. Econ. Paleontol. Mineral. Short Course* (eds) Staplin F L, Dow W G, Milner C W O, Milner C W D, Connor D I, Pocock S A J, van Gijzel P, Welte D H and Yukler M A **7** 133–157.
- El-Atfy H, Abeed Q, Uhd D and Littke R 2016 Palynology, palynofacies analysis, depositional environments and source rock potential of Lower Cretaceous successions in southern Iraq; *J. Mar. Pet. Geol.* **76** 362–376.
- El-Diasty W S, El Beialy S Y, Mostafa A R, El Adl H A and Batten D J 2017 Hydrocarbon source rock potential in the southwestern Gulf of Suez graben: Insights from organic geochemistry and palynofacies studies on well samples from the Ras El Bahar Oilfield; *J. Mar. Pet. Geol.* **80** 133–153.
- El-Khadragy A A, Shazly T F, Mousa D A, Ramadan M and Elsayy M Z 2018 Integration of well log analysis data with geochemical data to evaluate possible source rock. Case study from GM-ALEF-1 well, Ras Ghara oil Field, Gulf of Suez-Egypt; *Egypt. J. Petrol.* **27**(4) 911–918.
- Ercegovac M and Kostic A 2006 Organic facies and palynofacies: Nomenclature, classification and applicability for petroleum source rock evaluation; *Int. J. Coal Geol.* **68**(1) 70–78.
- Fazeelat T, Jalees M I and Bianchi T S 2010 Source rock potential of Eocene, Paleocene and Jurassic deposits in the subsurface of the Potwar Basin, northern Pakistan; *J. Pet. Geol.* **33**(1) 87–96.
- Filho M J G, De Oliveira A D, Da Silva F S, De Oliveira, Mendonça J, Rondon N F, Da Silva T F and Menezes T R 2012 Organic facies: Palynofacies and organic geochemistry approaches; In: *Earth's System Processes*, Intech Open Access Publisher.
- Ghasemi-Nejad E, Head M J and Naderi M 2009 Palynology and petroleum potential of the Kazhdumi Formation (Cretaceous: Albian–Cenomanian) in the South Pars field, northern Persian Gulf; *J. Mar. Pet. Geol.* **26**(6) 805–816.
- Golonka J 2007 Late Triassic and Early Jurassic palaeogeography of the world; *Palaeogeogr. Palaeoclimatol. Palaeoecol.* **244**(1–4) 297–307.
- Grelaud S, Sassi W, De Lamotte D F, Jaswal T and Roure F 2002 Kinematics of eastern Salt Range and South Potwar Basin Pakistan; A new scenario; *J. Mar. Pet. Geol.* **19** 1127–1139.
- Hakimi M H, Abdullah W H, Shalaby M R and Alramisy G A 2014 Geochemistry and organic petrology study of Kimmeridgian organic-rich shales in the Marib–Shabowah Basin, Yemen: Origin and implication for depositional environments and oil-generation potential; *J. Mar. Pet. Geol.* **50** 185–201.

- Hakimi M H, Al-Matary A M and Hersi O S 2018a Late Jurassic bituminous shales from Marib oilfields in the Sabatayn Basin (NW Yemen): Geochemical and petrological analyses reveal oil-shale resource; *Fuel* **232** 530–542.
- Hakimi M H, Al-Matary A M and Hersi O S 2018b Burial and thermal history reconstruction of the Mukalla–Sayhut Basin in the Gulf of Aden, Yemen: Implications for hydrocarbon generation from Paleocene potential source rock; *J. African Earth Sci.* **144** 59–75.
- Hakimi M H, Abdullah W H, Hersi O S, Lashin A A, El Alfy M M, Makeen Y M and Hatem B A 2019 Organic geochemistry of the Early Cretaceous shales, Saar Formation in the East Shabwah oil fields, onshore Masila Basin of eastern Yemen; *J. Pet. Sci. Eng.* **179** 394–409.
- Hakimi M H, Ahmed A, Kahal A Y, Hersi O S, Al Faifi H J and Qaysi S 2020 Organic geochemistry and basin modeling of Late Cretaceous Harshiyat Formation in the onshore and offshore basins in Yemen: Implications for effective source rock potential and hydrocarbon generation; *J. Mar. Pet. Geol.* **122** 104701.
- Huang W B, Salad Hersi O, Lu S F and Deng S W 2017 Quantitative modelling of hydrocarbon expulsion and quality grading of tight oil lacustrine source rocks: Case study of Qingshankou 1 member, central depression, Southern Songliao Basin China; *J. Mar. Pet. Geol.* **84** 34–48.
- Hunt J M 1995 *Petroleum Geochemistry and Geology*, 2nd edn, Freeman, San Francisco.
- Iqbal S, Jan I U, Akhter M G and Bibi M 2015 Palaeoenvironmental and sequence stratigraphic analyses of the Jurassic Datta Formation, Salt Range Pakistan; *J. Earth Syst. Sci.* **124**(4) 747–766.
- Iqbal S, Wagneich M, Jan I U, Kuerschner W M, Gier S and Bibi M 2019 Hot house climate during the Triassic/Jurassic transition: The evidence of climate change from the southern hemisphere Salt Range Pakistan; *Global Planet Change* **172** 15–32.
- Jan I U, Shah A, Stephenson M H, Iqbal S, Hanif M, Wagneich M and Hussain H S 2016 The sedimentology of the Lower Permian Dandot Formation: A component of the Gondwana deglaciation sequence of the Salt Range, Pakistan; *Res. Paleontol. Stratigr.* **122**(1) 75–90.
- Jiang D X, Wang Y D, Robbins E I, Wei J and Tian N 2008 Mesozoic non-marine petroleum source rocks determined by palynomorphs in the Tarim Basin, Xinjiang, northwestern China; *Geol. Mag.* **145**(06) 868–885.
- Kadri I B 1995 *Petroleum Geology of Pakistan*, Pakistan Petroleum Limited, Karachi.
- Kazmi A H and Abbasi I A 2008 *Stratigraphy and historical geology of Pakistan*; Department & National Centre of Excellence in Geology, University of Peshawar, Peshawar, Pakistan.
- Kazmi A H and Jan M Q 1997 *Geology and tectonics of Pakistan*; Graphic Publisher, Karachi, pp. 130–142.
- Khan N 2016 Hydrocarbon source rock potential evaluation of the Early Jurassic Datta Formation Salt Range, Pakistan; MS Thesis, National Centre of Excellence in Geology, University of Peshawar, Pakistan.
- Khan N, Anjum N, Ahmad M, Awais M and Ullah N 2018 Hydrocarbon source rock potential evaluation of the Late Paleocene Patala Formation, Salt Range Pakistan: Organic geochemical and palynofacies approach; *J. Earth Syst. Sci.* **127** 98–116.
- Koch G, Prtoljan B, Husinec A and Hajek Tadesse V 2017 Palynofacies and paleoenvironment of the Upper Jurassic mud-supported carbonates, southern Croatia: Preliminary evaluation of the hydrocarbon source rock potential; *J. Mar. Pet. Geol.* **80** 243–253.
- Kuerschner W M, Iqbal S, Wagneich M, Jan I and Gier S 2017 Palynology and carbon isotope stratigraphy of the Triassic–Jurassic transition in the Salt Range Pakistan; In: *EGU General Assembly Conference Abstract* **19** 15291.
- Mertmann D 2003 Evolution of the marine Permian carbonate platform in the Salt Range Pakistan; *Palaeogeogr. Palaeoclimatol. Palaeoecol.* **191**(3–4) 373–384.
- Mujtaba M and Memon A M 1990 Diagenesis and pore space development of Datta Sandstones in Salt Range and Surghar Range Pak; *J. Hydrocarb. Res.* **2** 57–66.
- Naeher S, Hollis C J, Clowes C D, Ventura G T, Shepherd C L, Crouch E M and Sykes R 2019 Depositional and organofacies influences on the petroleum potential of an unusual marine source rock: Waipawa Formation (Paleocene) in southern East Coast Basin, New Zealand; *J. Mar. Pet. Geol.* **104** 468–488.
- Pacton M, Gorin G E and Vasconcelos C 2011 Amorphous organic matter – Experimental data on formation and the role of microbes; *Rev. Palaeobot. Palynol.* **166**(3) 253–267.
- Pandey D K, Choudhary S, Bahadur T J, Swami N, Poonia D and Sha J 2012 A review of the Lower- lowermost Upper Jurassic facies and stratigraphy of the Jaisalmer Basin, western Rajasthan, India; *Volumina Jurassica* **10**(10) 61–82.
- Pandey R, Kumar D, Maurya A S and Pandey P 2019 Hydrocarbon generation potential of source rocks in Jaisalmer Basin, Rajasthan, India; *Curr. Sci.* **116**(5) 822.
- Peters K E 1986 Guidelines for evaluating petroleum source rock using programmed pyrolysis; *Am. Assoc. Pet. Geol. Bull.* **70**(3) 318–329.
- Pross J, Pletsch T, Shillington D J, Ligouis B, Schellenberg F and Kus J 2007 Thermal alteration of terrestrial palynomorphs in mid-Cretaceous organic-rich mudstones intruded by an igneous sill Newfoundland Margin, ODP Hole 1276A; *Int. J. Coal Geol.* **70**(4) 277–291.
- Rai J, Bajpai S, Kumar R, Singh A, Kumar K and Prakash N 2016 The earliest marine transgression in western India: New insights from calcareous nannofossils from Lathi Formation Jaisalmer Basin; *Curr. Sci.* **111**(10) 1631–1639.
- Rees P M, Ziegler A M, Valdes P J, Huber B T, Macleod K G and Wing S L 2000 Jurassic phytogeography and climates: New data and model comparisons; In: *Warm Climates in Earth History*, pp. 297–318.
- Schneider A C, Mutterlose J, Blumenberg M, Heimhofer U and Luppold F W 2019 Palynofacies, micropalaeontology, and source rock evaluation of non-marine Jurassic Cretaceous boundary deposits from northern Germany: Implications for palaeoenvironment and hydrocarbon potential; *J. Mar. Pet. Geol.* **103** 526–548.
- Shah S M I 2009 *Stratigraphy of Pakistan*; 22nd edn, Govt. Pak. Ministry of Petrol. & Nat; Resour. Geol. Surv. Karachi, Pakistan.
- Traverse A 2007 Paleopalynology; In: *Topics in Geobiology*, 2nd edn, Springer, Dordrecht, The Netherlands.
- Tucker M E 2003 *Sedimentary Rocks in the Field*, John Wiley & Sons.

- Tyson R V 1995 *Sedimentary organic matter: Organic facies and palynofacies*; Chapman and Hall, London.
- van Krevelen D W 1993 *Coal: Typology-Physics-Chemistry-Constitution*; 3rd edn. Elsevier Science, Amsterdam.
- Wandrey C J, Law B E and Shah H A 2004 Patala-Nammal composite total petroleum system, Kohat-Potwar geologic province, Pakistan, United States (US) Department of the Interior; *US Geol. Surv. Bull.* **2208** C2-10.
- Zadan K and Arbab K A 2015 A review on lithostratigraphy and biostratigraphy of Jaisalmer Basin, Western Rajasthan, India; *Int. Res. J. Earth Sci.* **3** 37-45.
- Zaidi S N A, Brohi I A, Ramzan K, Ahmed N, Mehmood F and Brohi A 2013 Distribution and hydrocarbon potential of Datta sands in Upper Indus Basin, Pakistan; *Sindh Univ. Res. J. Sci. Ser.* **45(2)** 325-332.
- Zhang M, Ji L, Wu Y and He C 2015 Palynofacies and geochemical analysis of the Triassic Yanchang Formation, Ordos Basin: Implications for hydrocarbon generation potential and the paleoenvironment of continental source rocks; *Int. J. Coal Geol.* **152** 159-176.
- Zhao Z, Pang X, Jiang F, Wang K, Li L, Zhang K and Zheng X 2018 Hydrocarbon generation from confined pyrolysis of Lower Permian Shanxi Formation coal and coal measure mudstone in the Shenfu area, northeastern Ordos Basin China; *J. Mar. Pet. Geol.* **97** 355-369.
- Zoba M K, El Beialy S Y, El Sheikh H A and El Beshtawy M K 2013 Jurassic-Cretaceous palynomorphs, palynofacies, and petroleum potential of the Sharib 1x and Ghoroud 1x wells, north Western Desert Egypt; *J. Afr. Earth Sci.* **78** 51-65.

Corresponding editor: SANTANU BANERJEE